PHYSICAL REVIEW A VOLUME 47, NUMBER 2 FEBRUARY 1993

Electron correlation in the continuum: The e-2e process for small relative momenta of the outgoing electrons

Pan Guang-yan,* Preben Hvelplund, and Helge Knudsen
Institute of Physics and Astronomy, University of Aarhus, DK-8000 Aarhus C, Denmark

Yasunori Yamazaki
Institute of Physics, College of Arts and Sciences, University of Tokyo, Komaba, Meguro-Ko, Tokyo 153, Japan

Michael Brauner
Department of Physics and Astronomy, University of Tennessee, Knoxville, Tennessee 37996

John S. Briggs
Fakultät für Physik, Albert-Ludwigs Universität Freiburg, D-7800 Freiburg, Germany
(Received 15 September 1992)

We present measured triply differential cross sections for the ejection of two electrons into the forward direction following impact of 400-, 600-, and 1000-eV electrons on helium atoms. The coplanar, symmetric geometry was used with a scattering angle of 4°. A comparison with our theoretical calculations demonstrates the clear effect of the final-state electron-electron correlation in fast electron-atom ionizing collisions.

PACS number(s): 34.80.Dp

Continuum states of particles interacting through Coulomb forces present a great challenge theoretically since, unlike the situation for short-range forces, the motion of the particles remains correlated out to infinite separation. In the case of electron-impact ionization of atoms the usual approach is based upon the separate motion of the two electrons in the field of the residual positively charged ion. The electron-electron interaction is then included in some approximate way, e.g., by the use of effective charges for the electron-nucleus interaction. This is analogous to the use of an independent-particle basis to describe bound states, with electron correlation included in a second step. However, in bound states an implicit average is made over all relative momenta of the two electrons. In continuum states each state of relative momentum can be measured separately. In the case of electron-hydrogen atom impact at energies just above the three-body break-up threshold (i.e., tens of electron volts of total energy) it is clear that all relative momenta are small. Then all three two-body interactions should be treated on an equal footing. A final-state wave function with this property [1] has been applied to the calculation of triply differential cross sections (TDCS's) and a strong repulsive effect between the two electrons observed experimentally has been confirmed. The importance of the electron-electron repulsion was also demonstrated by Botero and Macek [2]. It has been shown [3] that this same repulsion effect is important even at high energies (hundreds of eV total energy) and even when one electron has low momentum and the other has high momentum with respect to the nucleus. This is a clear manifestation of electron correlation in the continuum arising from the infinite range of the Coulomb force.

As yet no experiments have been performed at high energies in which the relative angle of the two outgoing electrons is small. Preliminary calculations [3] predict a minimum under these conditions: the TDCS's converging exponentially to zero as the relative momentum of the two electrons tends to zero. Here we report measurements and calculations which confirm the existence of this exponentially converging TDCS.

The major reason for the existence of a vanishing TDCS for electron momenta $\mathbf{k}_a = \mathbf{k}_b$ can be traced to the occurrence of a Coulomb density of states (CDS) factor in the three-body continuum wave function [3]. The same factor has been shown to give a linear divergence in the TDCS in the case of positive ions [4] as projectiles when the ionized electron has the same velocity as the projectile in the final state. When integrated over a finite acceptance angle a cusp appears in the TDCS [5]. Such cusps have been well studied both experimentally and theoretically. Here we confirm the analogous effect on the TDCS for electron impact. It should also be mentioned that a similar effect is predicted [6] to occur in TDCS's for antiproton impact although to date no precise measurements exist.

The theory used in this paper is described in detail in Brauner, Briggs, and Broad [7]. Here we only give a short overview. In the incident channel two electrons called e_1 and e_b and the nucleus with charge $Z_T = 2$ are bound to form the helium atom. The electron e_a is free. The triply differential cross section for coplanar geometry is given by

$$\frac{d\sigma}{d\theta_a d\theta_b dE_b} = 2(2\pi)^4 \frac{k_a k_b}{K_i} |T_{fi}|^2 , \quad (1)$$

where $\mathbf{K}_i$ is the momentum of the incoming electron e_a

and $\mathbf{k}_a$ and $\mathbf{k}_b$ are the momenta of the free electrons e_a and e_b after the scattering. The T matrix is defined as

$$T_{fi}=\langle \Psi_f^- | V_i | \Phi_i \rangle \tag{2}$$

with the perturbation V_i being that part of the total interaction not diagonalized in the initial state. The initial wave function Φ_i is a product of a plane wave describing the incoming projectile electron e_a and the ^1S helium bound state Φ_{He} which is a product of $1s$ hydrogenic wave functions [8]

$$\Phi_{\mathrm{He}}=\frac{Z_S^3}{\pi}\exp[-Z_S(r_1+r_b)] \tag{3}$$

with the Slater charge

$$Z_S=Z_T-\tfrac{5}{16}=1.6875\ . \tag{4}$$

The two free electrons and the He^+ ion in the final channel are described by a product of a He^+ $1s$ wave function

$$\Phi_{\mathrm{He}^+}=\left[\frac{Z_T^3}{\pi}\right]^{1/2}\exp(-Z_T r_1) \tag{5}$$

and a three-particle wave function

$$\begin{aligned}\Psi_3^{-1}=&(2\pi)^{-3/2}\exp(i\mathbf{k}_a\cdot\mathbf{r}_a)\exp(-\pi\alpha_a/2)\Gamma(1-i\alpha_a)\,{}_1F_1(i\alpha_a;1;-i[k_a r_a+\mathbf{k}_a\cdot\mathbf{r}_a])\\ &\times(2\pi)^{-3/2}\exp(i\mathbf{k}_b\cdot\mathbf{r}_b)\exp(-\pi\alpha_b/2)\Gamma(1-i\alpha_b)\,{}_1F_1(i\alpha_b;1;-i[k_b r_b+\mathbf{k}_b\cdot\mathbf{r}_b])\\ &\times\exp(-\pi\alpha_{ab}/2)\Gamma(1-i\alpha_{ab})\,{}_1F_1(i\alpha_{ab};1;-i[k_b r_{ab}+\mathbf{k}_{ab}\cdot\mathbf{r}_{ab}])\ .\end{aligned} \tag{6}$$

Here $\mathbf{r}_{ab}$ and $\mathbf{k}_{ab}$ are the relative distance and momentum of the two free electrons and the Sommerfeld parameters have the following form:

$$\alpha_a=-1/k_a\ , \tag{7}$$

$$\alpha_b=-1/k_b\ , \tag{8}$$

$$\alpha_{ab}=1/(2k_{ab})\ . \tag{9}$$

This three-body Coulomb wave function (3C) has the correct asymptotic Coulomb behavior.

For comparison we will also present calculations in which the wave function (6) is simplified to include only the two Coulomb wave functions (2C) between the ionized electrons and the He^+ ion, the electron-electron repulsion factor in (6) being replaced by unity. The TDCS using plane waves only (PW) in the final state will be shown also.

Since the primary aim of the present experiment is to investigate the TDCS near a combination of ejected energies and angles $E_a, E_b, \theta_a, \theta_b$ where we expect the TDCS to vanish, our apparatus has been designed with large solid angles $\Delta\Omega_a$, $\Delta\Omega_b$ and energy acceptances ΔE_a, ΔE_b. The setup is shown schematically in Fig. 1. It is placed inside a long μ-metal tube which reduces the residual magnetic field to a magnitude less than 10 mG.

The electron beam is produced by a well-aligned, conventional television-tube electron gun. Typically, the electron current was 1 nA. The beam passed through a $l=20$-mm-long gas cell connected to a Pirani gauge. Typical target gas pressures were less than 1 mTorr. The electron gun and the gas cell were differentially pumped by a diffusion pump, while the vacuum of the rest of the chamber was maintained by a turbomolecular pump. Typically, the overall pressure was around 10^{-6} Torr. The electron beam was detected downstream by a properly biased Faraday cup; 150 mm downstream from the center of the gas cell were two symmetrically placed, rectangular apertures, each 8 mm wide in the scattering plane and 10 mm wide perpendicular to it. Electrons entering these apertures were energy analyzed by two electrostatic analyzers of cylindrical sector field 64° geometry, having a plate distance of 8 mm and a central orbit radius of 60 mm. After each analyzer, a rectangular energy-defining aperture of 3×10 mm width permitted the electrons to impinge on a ceramic channeltron detector. Dependent on the analyzed energy, the Ceratron cone voltage was adjusted so that the impact energy was always the same. This means that the Ceratron detection efficiencies were fixed.

Seen from the center of the gas cell, the mean, accepted scattering angle for each detector system was $\theta_a=\theta_b=4°$ in the scattering plane, while the scattering angle perpendicular to the scattering plane was restricted to less than 1.3°. The acceptance solid angle was $\Delta\Omega_a=\Delta\Omega_b=2.35$ msr.

The signals from the detectors were fed to standard fast electronics, and then, after a proper time delay of one

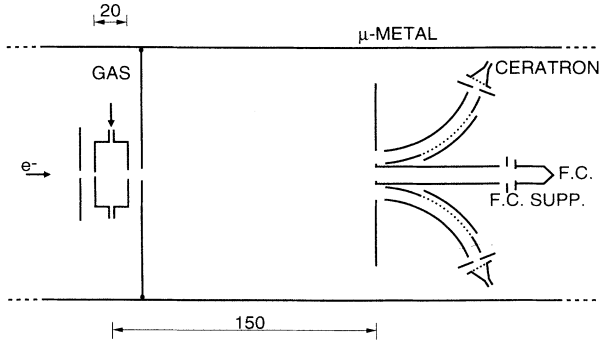

FIG. 1. Here is shown schematically the experimental apparatus. FC denotes the Faraday cup and FC SUPP denotes the electron suppressor. Measures are in mm. The exit and entrance apertures of the gas cell are 3- and 1-mm diameter, respectively.

channel, to a time-to-amplitude converter (TAC). Counting times varied from hours to days. The resulting TAC spectra contain a narrow coincidence peak and a flat background. Typically, the signal-to-background ratio was 0.2–0.5. By subtracting the random contribution from the peak content, the number of coincidences $N_{\rm co}$ is achieved. For each run, one analyzer was set at an energy E_a. Then several TAC spectra were obtained, with the other analyzer set at a range of energies close to and at $E_b = E - E_i - E_a$, where E is the projectile energy, and E_i is the target atom ionization potential. Invariantly, the largest $N_{\rm co}$, and the value used in the following analysis, was obtained at E_b. The triply differential cross section was obtained from

$$\frac{d^3\sigma}{d\Omega_a d\Omega_b dE_b} = \frac{N_{\rm co}}{nN_e[l\Delta\Omega_a\Delta\Omega_b]_{\rm eff}\epsilon_a\epsilon_b\Delta E_{\rm co}} , \quad (10)$$

where n is the target gas density, N_e the accumulated number of beam electrons, $[l\Delta\Omega_a\Delta\Omega_b]_{\rm eff}$ the effective value of the product of gas cell length and detection solid angles, ϵ_a and ϵ_b the detection efficiencies, and finally, $\Delta E_{\rm co}$ is the coincidence energy resolution. As the TDCS near the minimum is *very* small, multiple collisions might result in spurious signals. We therefore kept the target pressure very low, and took care to check that our measured TDCS's [Eq. (10)] were independent of the target gas density.

Since we aim to investigate the shape of the minimum rather than the absolute magnitude of the cross section, we have refrained from a detailed measurement of the factors in the denominator of Eq. (10). Instead, we have estimated their magnitude as follows. The gas cell length was taken to be the geometric 20 mm. The solid angles vary depending on the position of the collision in the gas cell, but were set at the mean, geometric value mentioned above. The product of gas cell length and the detector solid angles is a constant, since we do not vary the scattering angles. From the geometry of our analyzers, we calculate the largest acceptable deviation from the mean energy E to be $\Delta E = 0.0122E$, so that the full width of the energy resolution function is $\Delta E_a = 0.0244E_a$ and likewise for the other detector system. Following Lahman-Benanni *et al.* [9], we then find the coincidence energy resolution $\Delta E_{\rm co}^{-2} = \Delta E_a^{-2} + \Delta E_b^{-2}$. The transmission of the grids in front of the Ceratrons was 0.8. Using a "standard" curve of Ceratron efficiencies [10], we then find that $\epsilon_a\epsilon_b = 0.21$.

Of course, the above estimates are rather crude. However, it is reassuring that the value of the experimental TDCS's, which we obtain by applying them in Eq. (10), is the same as the ones we would obtain by normalizing our data to the theoretical TDCS at $E_b = 7$ a.u. for 1000-eV impact on helium as calculated by the 3C method described previously.

The experimental TDCS data for 400-, 600-, and 1000-eV electrons on helium are compared with the theoretical results in Figs. 2(a)–2(c). Although there is some discrepancy between the 3C theoretical result and the experimental data, it is clear that this calculation, which takes fully into account the electron-electron repulsion in the final state, describes the experimental data much better than do the 2C (or PW) theoretical results, for which the electron-electron interaction in the final state is not included.

The deep minimum at $E_a = E_b$ in Fig. 2 can mainly be explained by the Coulomb interaction of the two outgoing electrons. The electron-electron Coulomb normalization factor

$$|\exp(-\pi\alpha_{ab}/2)\Gamma(1-i\alpha_{ab})|^2 = \frac{2\pi\alpha_{ab}}{\exp(2\pi\alpha_{ab})-1} \quad (11)$$

of Eq. (6) vanishes exponentially for vanishing relative

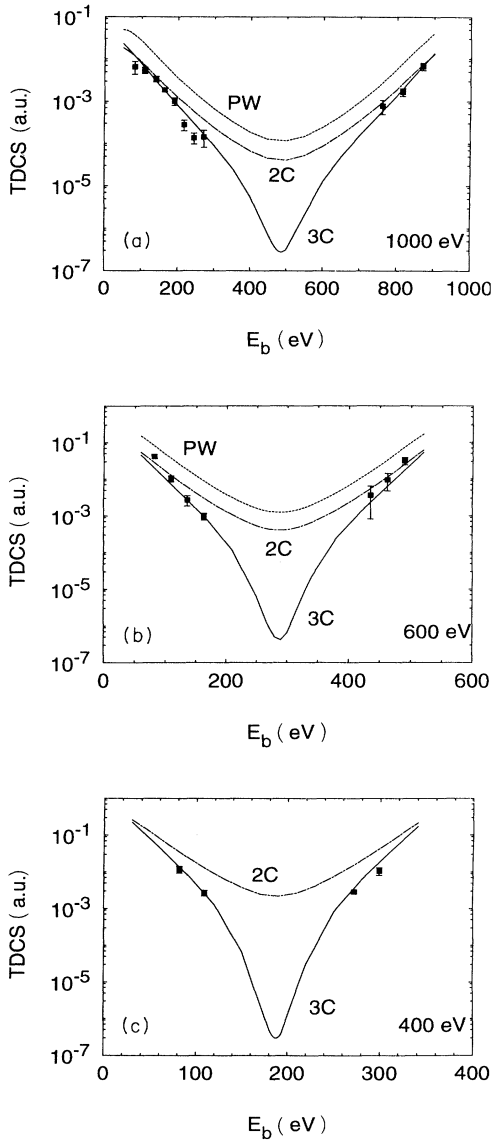

FIG. 2. The TDCS for (a) 1000-eV, (b) 600-eV, and (c) 400-eV electrons on helium at $\theta_a = \theta_b = 4°$. The abscissas show E_b, while $E_a = E - E_i - E_b$. The curves show the results of the present theoretical calculations based on the PW, 2C, and 3C models.

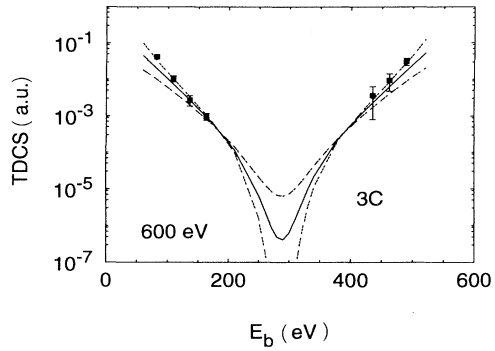

FIG. 3. The experimental TDCS for 600-eV impact compared with the 3C theoretical result calculated for $\theta_a = \theta_b = 2.3°$ (dot-dashed line), 4° (solid line), and 5.9° (dashed line).

momentum $\mathbf{k}_{ab}$, which has been predicted for antiproton impact [6] and for electron impact [3]. Because of the Pauli principle the antisymmetrized 2C and PW wave functions produce also a relative minimum at $E_a = E_b$. However, the experiments clearly show that one needs the 3C wave function (6) and especially the electron-electron normalization factor to explain the deep minimum at $E_a = E_b$.

The scattering angles θ_a and θ_b vary as a function of the position of the collision in the gas cell. Furthermore, the defining rectangular apertures in front of the Ceratron detectors allow a rather large variation in scattering angle. Actually, although we give the *mean* scattering angle as 4°, the scattering angles may vary from 2.3° to 5.9°. We realize that since the TDCS varies nonlinearly with scattering angle, we may thus introduce some systematic error into a comparison with the theoretical calculations. However, as can be seen in Fig. 3, where the 600-eV experimental data are compared with the 3C theory calculated for 2.3°,4°, and 5.9° scattering angle, the rather large range of scattering angles accepted experimentally does not obscure the conclusion reached above.

The authors would like to acknowledge the expert help in the laboratory by Poul Aggerholm. The work was partially supported by the DFG through Grant No. SFB276.

*Permanent address: Institute of Physics, Chinese Academy of Sciences, Beijing, P.R. China.

[1] M. Brauner, J.S. Briggs, H. Klar, J. T. Broad, T. Rösel, K. Jung, and H. Ehrhardt, J. Phys. B **24**, 657 (1991).
[2] J. Botero and J. H. Macek, Phys. Rev. Lett. **68**, 576 (1992).
[3] M. Brauner and J. S. Briggs, J. Phys. B **19**, L325 (1986).
[4] J. Macek, Phys. Rev. A **1**, 235 (1970).
[5] K. Dettmann, K. G. Harrison, and M. W. Lucas, J. Phys. B **7**, 269 (1974).
[6] C. R. Garibotti and J. E. Miraglia, Phys. Rev. A **21**, 572 (1980).
[7] M. Brauner, J. S. Briggs, and J. T. Broad, J. Phys. B **24**, 287 (1991).
[8] H. A. Bethe and E. E. Salpeter, *Encyclopedia of Physics*, edited by S. Flügge (Springer, Berlin, 1957), Vol. XXXV, p. 204.
[9] A. Lahmam-Bennani, H. F. Wellenstein, A. Duguet, and M. Lecas, Rev. Sci. Instrum. **56**, 439 (1985).
[10] D. de Bruijn, P. van Deenen, D. Dijkkamp, H. Holsboer, and C. van Oven, Technical Report No. 54.246a FOM Institute, Amsterdam, Holland, 1982 (unpublished).